

Short-term Associations between Accumulated Rainfall and Atmospheric Moisture during Landfall of Three Atlantic Hurricanes

Peng Jia

Department of Geography and Anthropology

Louisiana State University

Baton Rouge, LA 70803

E-mail: rs.jiapeng@gmail.com

Andrew Joyner

Department of Geosciences

East Tennessee State University

Johnson City, TN 37604

Yilun Sun

St. Jude Children's Research Hospital

Memphis, TN 38105

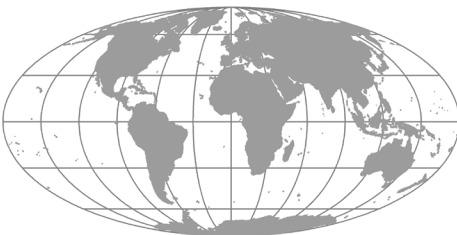
ABSTRACT

Most hurricane-related deaths are caused by flooding and, as a result, accurate forecasting of rainfall can have a profound impact on reducing loss of life as well as property damages resulting from hurricanes. Quantitative relationships between atmospheric moisture and rainfall have been examined during the landfall of three Atlantic hurricanes in the study, with Geographic Information System and high temporal resolution remote sensing data used and time lags between atmospheric moisture and rainfall taken into account. Results show that 1) atmospheric moisture and rainfall-related variables can be accurately gauged by satellite at any given place and provide approximate estimations for the average and total amounts of rainfall after three and six hours, and 2) the intensity of rainfall was weaker but lasted longer over land than over ocean.

Key Words: atmospheric moisture, rainfall, hurricane, GIS, forecast

INTRODUCTION

Hurricanes often produce substantial amounts of rainfall that can lead to widespread flooding (Tootle, Mirti and Piechota 2005) and these flood events are responsible for the majority of deaths associated with hurricanes (Elsberry 2002). Consequently, accurate forecasting of rainfall associated with hurricanes is crucial for reducing loss of life as well as property damages caused by hurricanes. In the Rainfall Climatology and Persistence model (R-CLIPER), utilized operationally in the Atlantic Ocean basin by the National Hurricane Center (NHC), the storm intensity has been considered the primary factor for hurricane rainfall forecasts (Jiang, Halverson and Zipser 2008). Moreover, there is a stronger statistical relationship found between accumulated rainfall (AR) and maximum wind intensity (MWI) before a hurricane makes landfall than there is after



landfall, which implies that the correlation between AR and MWI is stronger over ocean than over land (Jiang et al. 2008a). The effects of vertical wind shear and topography are taken into account and combined with the factors from R-CLIPER in a new model, named the Parametric Hurricane Rainfall Model (PHRaM) (Lonfat et al. 2007). The model assumes that the maximum AR over land is a function of satellite-derived rainfall potential over ocean prior to landfall, storm size, and translation speed; all variables found to be correlated with rainfall amounts (Jiang et al. 2008a).

In addition to inherent storm features, associated environmental parameters are also crucial in shaping the patterns of subsequent rainfall, such as the moisture budget (Carr and Bosart 1978; DiMego and Bosart 1982), total precipitable water (PWAT) (Jiang, Halverson and Zipser 2008), horizontal moisture convergence (HMC) (Jiang, Halverson and Simpson 2008; Jiang et al. 2008b) and ocean surface flux (OSF) (Jiang, Halverson and Zipser 2008). However, few statistical relationships between rainfall and environmental moisture during hurricanes have been documented (Jiang, Halverson and Zipser 2008).

An improvement in quantifying AR after combining PWAT, HMC, and OSF with MWI has also been found (Jiang, Halverson and Zipser 2008). However, no pronounced distinctions are found when combining only PWAT, rather than all three variables, with MWI. Owing to better measurability, the combination of PWAT and MWI creates a more practical prediction and greatly reduces the prediction error since HMC and OSF are model-derived parameters instead of satellite-derived observations (Jiang, Halverson and Zipser 2008).

Based on current research, few quantitative relationships between AR and PWAT have been studied for short-term forecast purposes. This study attempts to fill this gap by 1) utilizing moisture and rainfall data with high temporal resolution and 2) taking into account time lags between AR and PWAT,

to determine 1) if the amount of rainfall at the landfall of hurricanes was associated with the rainfall and moisture prior to landfall and 2) if that association varied depending on the location of the hurricane (i.e., over land or over water). A Geographic Information System (GIS) was utilized to pre-process spatial data of AR and PWAT, match different sources of data with a time lag, and create covariates for inclusion in statistical models. We examined three hurricanes (Frances, Ivan, and Jeanne) making landfall in the southeastern U.S.A. in September 2004.

STORM RECORDS

Frances made its first landfall over the southern end of Hutchinson Island near Stuart in the state of Florida at about 0430 UTC on 5th September 2004 as a Category 2 hurricane (90 knots maximum wind speed (MWS), according to the Saffir-Simpson Hurricane Wind Scale. It proceeded north-westward and emerged into the northeastern Gulf of Mexico early on 6th September, followed by a second landfall near the mouth of the Aucilla River in the Florida Big Bend region at about 1800 UTC with a MWS of 90 knots. Ivan made its initial landfall as a Category 3 hurricane (105 knots MWS) at approximately 0650 UTC on 16th September over the western end of Gulf Shores, Alabama, near its border with Florida. After landfall, Ivan tracked northeast across Alabama, along the border of Tennessee and North Carolina, then across Virginia, eventually emerging into the Atlantic Ocean near the Delmarva Peninsula in Virginia where it became an extra-tropical low around 1800 UTC on 18th September. Over the next three days, it moved south, then south-westward in the Atlantic Ocean and made a second landfall in Fort Lauderdale, Florida on the morning of 21st September at a MWS of 25 knots. Ivan eventually emerged over the southeastern Gulf of Mexico later that afternoon and made landfall in Cameron, Louisiana on 23rd September as a tropical depression. Jeanne, was similar to Frances in many ways: similar

landfall location on Hutchinson Island near Stuart, Florida, minimum central pressures (960 mb for Frances and 950 mb for Jeanne) and a similar track direction (crossing the coastline northwestward at about 280°). Jeanne made its only landfall at 0400 UTC on 26th September at a MWS of 105 knots, and moved across central Florida, Tampa and central Georgia over the next 36 hours, then continued moving northwards.

For our study period, we selected the 72 hours centered at the landfall time of each hurricane (36 hours prior to landfall and 36 hours after landfall). Since the coordinate locations of storm centers are only available every 6 hours (0000, 0600, 1200 and 1800 UTC¹) from Tropical Cyclone Reports by NHC, the time of landfall for each hurricane was approximated to the closest UTC hour. The study periods for Frances, Ivan and Jeanne are 1800 UTC on 3rd September to 1800 UTC on 6th September, 1800 UTC on 14th September to 1800 UTC on 17th September, and 1800 UTC on 24th September to 1800 UTC on 27th September, respectively. We only examined Ivan’s first landfall (near the Florida-Alabama border) for this study.

The MWS, representing MWI in this study, is defined as the total velocity gauged at the center of a hurricane combined with the storm’s speed of forward movement and vorticity. The maximum wind radius (MWR) is defined as the farthest extent of the hurricane wind field from the hurricane’s center measured at a given speed in all quadrants. This measurement produces an inexact representation, but is intended to reflect the expected size of storms with

a given speed and identify areas potentially affected by sustained winds at a given time. The extended best track data is utilized to estimate the MWR at 34-, 50- and 64-knot MWS (Demuth, DeMaria and Knaff 2006) (Table 1). Due to a dearth of knowledge on the relationships between wind and rain fields, we assumed 111 km as a conservative estimate for the radius of the inner core of the hurricanes, as well as 333 km for the average radius of the entire hurricane environment.

METEOROLOGICAL DATA

To represent the AR on the ground, we selected the 3-hourly Tropical Rainfall Measuring Mission (TRMM) and Other Rainfall Estimate (3B42 dataset, version 6) with a 32.2×32.1 km² spatial resolution, which is a combined product based on two different sets of sensors: microwave and infrared (IR). In the current TRMM 3B42 system, passive microwave observations from TMI, AMSR-E and SSM/I are converted to the precipitation estimates with sensor-specific versions of the Goddard Profiling Algorithm (GPROF) (Kummerow, Olson and Giglio 1996; Olson et al. 1999).

PWAT is the depth of liquid water that would result after precipitating all of the water vapor in a vertical column over a given location and was utilized as an indicator for atmospheric moisture in this study. We derived PWAT data in 3-hourly increments with a 21.4×27.8 km² spatial resolution from the North American Regional Reanalysis (NARR) dataset, the temporal and spatial resolution of which were higher than of those

Table 1. Range of maximum wind radii (MWR) in all quadrants of given wind speeds, in kilometers

Landfall	34-knot	50-knot	64-knot
Frances (1st)	231.5 – 324.1	138.9 – 231.5	74.08 – 138.9
Frances (2nd)	0 – 166.68	0 – 46.3	0
Ivan (1st)	138.9 – 463	74.08 – 231.5	46.3 – 83.34
Ivan (2nd)	0	0	0

calculated from the Navy Operational Global Atmospheric Prediction System (NOGAPS) analysis with 12-hour temporal resolution and a $111 \times 111 \text{ km}^2$ spatial resolution.

METHODS

Kriging is a geostatistical interpolation technique that is used to predict values at unobserved locations based on their observed counterparts at nearby locations (Oliver and Webster 1990). More weight is given to observed values that are closest to the unobserved locations and spatial arrangement and directionality can be utilized to improve predictions. Because of the weighting method utilized by Kriging, estimation error is minimized and a continuous surface is produced from a set of discrete points (Akala, Devabhaktuni and Kumar 2010; Li and Revesz 2004). During Kriging analysis, the value for a given location uses neighboring values based on a range of correlation where values farther away are less correlated than values that are closest. The range of correlation reaches a "sill" and values beyond the sill are no longer incorporated into calculations. Calculations are based on the degree of spatial autocorrelation and regionalized variable theory (Oliver and Webster 1990). The quality of interpolated values depends on the spatial variation of the phenomenon and distribution of known points. Both atmospheric moisture and precipitation are typical continuous phenomena, and PWAT and AR datasets used in this study are both evenly-distributed gridded data. Therefore, we used ordinary Kriging with a spherical semi-variogram model for the dataset of AR and PWAT in *ArcGIS* 10.0 (ESRI 2010). The semi-variogram represents the correlation matrix between observed values and predicted values and incorporates the range and sill during the modeling process.

Given that the temporal resolution of AR and PWAT data was 3 hours, we hypothesized a time lag of three or six hours between the occurrences of AR and PWAT at a given location. A series of points were created for

the storm center at different moments (0000, 0600, 1200 and 1800 UTC) (Fig. 1). We produced buffer zones with radii of 111 km and 333 km based on the storm centers. As a result, each point with an inner (111 km) and outer area (333 km) around it corresponded to an exclusive arrival time of storm centers (0000, 0600, 1200 or 1800 UTC), depending on when the storm center moved to that point. Then we averaged all values of AR (avgIAR) and PWAT (avgIPW) within each inner area at their own arrival time, as well as within each outer area (avgOAR and avgOPW). We also added all values of AR and PWAT together within each inner (sumIAR and sumIPW) and outer area (sumOAR and sumOPW). In addition, the values of AR and PWAT three and six hours prior to and immediately after the arrival time were averaged and added together within each inner/outer area, resulting in a series of variables shown in Table 2.

Regression analysis models the relationships between a dependent variable and one or more independent variables to assess the extent to which a dependent variable is affected by one explanatory variable (bivariate) or a combination of independent variables (multivariate). Stepwise regression employs a screening procedure to determine which explanatory variables are retained and dropped from the model based on their explanatory power by setting a certain threshold of probability, or F-statistic. It is a sequential method for adding and removing regressors to determine a final regression model that provides the best possible fit.

There are four types of stepwise procedures: forward stepwise (FS), backward stepwise (BS), general stepwise (GS), and minimum mean-square error stepwise (MMSES), of which the FS regression, starting with a full model including all regressors, was selected in this study. FS regression initially seeks the variable that explains the greatest amount of variation in the dependent variable. If the p -value is lower than the threshold, it is added into the model. Then it continues seeking the variable providing the next greatest amount of explanatory power to the model based on

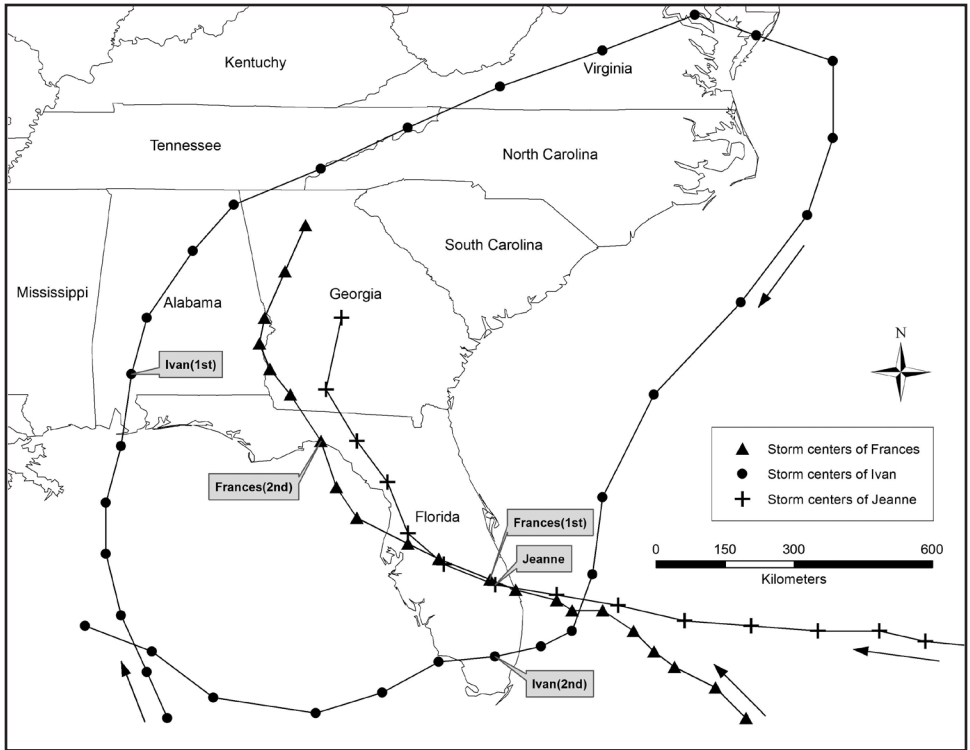


Figure 1. Storm center locations of three hurricanes (Frances, Ivan, and Jeanne).

the unexplained variation, and the p -value would decide if it is added into or removed from the model. The process is repeated until no qualified variables are left out of the model.

The F-ratio, computed as the ratio of the explained to unexplained variation, adjusted R^2 value, and p -value collectively assess the explanatory power provided by all independent variables left in the model. Additionally, we used a combination of the Kolmogorov-Smirnov (K-S), Shapiro-Wilk (S-W), and Anderson-Darling (A-D) tests to evaluate the normality of error, which plays a critical role in assessing the structure and significance of our regression models. The K-S test is often used to determine if the current group of samples comes from a completely specified continuous distribution. The S-W test is used when the number of observations ranges from 3 to 5000. The A-D test is particularly useful when the number of observations is

between 25 and 40 because it is less likely to incorrectly reject the assumption of normality with a smaller sample size. However, the A-D test can also be used for larger sample sizes so it was used to complement other tests by providing a greater degree of certainty.

The repeated measurement deals with response outcomes measured on the same experimental unit at different times or under different conditions (Inc. 1999). In this study, we calculated means and sums of the same factors, AR and PWAT, five times within each inner/outer area at varying intervals: arrival time of storm centers and three and six hours prior to and immediately after the arrival time. SAS PROC MIXED is a powerful and flexible variance procedure with the capacity for analyzing many different types of complex statistical data, including repeated measures data (Moser 2004). The repeated measures analysis was undertaken

Table 2. Definitions of each variable utilized in the regression analysis.

Variable	Definition
avgARlb6/ avgPWlb6	Average AR/PWAT within an inner area 6 hours before the arrival of storm centers
avgAROb6/ avgPWOOb6	Average AR/PWAT within an outer area 6 hours before the arrival of storm centers
sumARlb6/ sumPWlb6	Accumulated AR/PWAT within an inner area 6 hours before the arrival of storm centers
sumAROb6/ sumPWOOb6	Accumulated AR/PWAT within an outer area 6 hours before the arrival of storm centers
avgARlb3/ avgPWlb3	Average AR/PWAT within an inner area 3 hours before the arrival of storm centers
avgAROb3/ avgPWOOb3	Average AR/PWAT within an outer area 3 hours before the arrival of storm centers
sumARlb3/ sumPWlb3	Accumulated AR/PWAT within an inner area 3 hours before the arrival of storm centers
sumAROb3/ sumPWOOb3	Accumulated AR/PWAT within an outer area 3 hours before the arrival of storm centers
avgARI/ avgPWI	Average AR/PWAT within an inner area at the arrival time of storm centers
avgARO/ avgPWO	Average AR/PWAT within an outer area at the arrival time of storm centers
sumARI/ sumPWI	Accumulated AR/PWAT within an inner area at the arrival time of storm centers
sumARO/ sumPWO	Accumulated AR/PWAT within an outer area at the arrival time of storm centers
avgARla3/ avgPWla3	Average AR/PWAT within an inner area 3 hours after the arrival of storm centers
avgAROba3/ avgPWOa3	Average AR/PWAT within an outer area 3 hours after the arrival of storm centers
sumARla3/ sumPWla3	Accumulated AR/PWAT within an inner area 3 hours after the arrival of storm centers
sumAROba3/ sumPWOa3	Accumulated AR/PWAT within an outer area 3 hours after the arrival of storm centers
avgARla6/ avgPWla6	Average AR/PWAT within an inner area 6 hours after the arrival of storm centers
avgAROba6/ avgPWOa6	Average AR/PWAT within an outer area 6 hours after the arrival of storm centers
sumARla6/ sumPWla6	Accumulated AR/PWAT within an inner area 6 hours after the arrival of storm centers
sumAROba6/ sumPWOa6	Accumulated AR/PWAT within an outer area 6 hours after the arrival of storm centers

by the PROC MIXED procedure in SAS 9.3 (SAS Institute Inc, Cary, NC) to determine the relationship between AR and PWAT over time, and whether the amount of rainfall is affected by landfall.

RESULTS

The locations of storm centers are available in 6-hour increments during the 72-hour

study period centered at the landfall time, so 13 inner/outer areas should be created for each landfall. However, since the interval between the two landfalls of Frances is only 36 hours, the 36 hours after the first landfall and before the second landfall were identical. Thus, we ended up with 19 inner/outer areas for Frances, 26 for Ivan and 13 for Jeanne, for a total of 58 records to be included in the regression analysis. The average

and total amounts of accumulated rainfall within inner/outer areas at the arrival time of each storm at the 6-hour interval locations (avgARI, avgARO, sumARI and sumARO) and at three hours (avgARiA3, avgAROA3, sumARiA3 and sumAROA3) and six hours after the arrival time at each 6-hour interval location (avgARiA6, avgAROA6, sumARiA6 and sumAROA6) were treated as dependent variables. Independent variables in different models varied, including the MWS at the arrival time of storm centers, and all AR- and PWAT-related variables occurring three and six hours after the moment when the dependent variable occurred. The basic statistics of averaged AR- and PWAT-related variables within inner areas are shown in Table 3. Larger amounts of average AR within inner areas occurred three hours prior to and after the arrival time of storm centers, and additionally, larger amounts of average PWAT were reported six hours prior to and at the arrival time of storm centers, which implies that the hypothesized 3-hour time lag was reasonable.

Regression results when using only MWS as an independent variable are shown in Table 4. The average and total amounts of AR within inner areas, measured at the arrival time of storm centers, even after three and six hours, were all significantly positively

correlated with MWS at the arrival time. When integrating all AR- and PWAT-related variables with MWS, the results for the AR within inner areas at different moments are shown in Table 5, 6 and 7, respectively. The best models for each dependent variable, with the highest adjusted R^2 /F-ratio and all three tests of normality passed, are highlighted in the tables. The comparison of adjusted R^2 values is compiled in Table 8, where it appears that, since involving AR- and PWAT-related variables in the models, the variations are well-explained for all dependent variables except the total AR at the arrival time of storm centers.

As the best models indicated, when the storm center arrived at a given location, the average amount of AR within the inner area centered at the given location was influenced by not only MWS at that time, but also the average AR and PWAT three hours prior within that area (avgARiB3 and avgPWiB3). The total amount of AR was still better predicted by MWS alone. Three hours after the storm passed a given location, both the average and total amounts of AR within that area were better estimated by the total amount of AR at the arrival time (sumARI), namely, three hours prior. After six hours when the storm center passed a given location, the MWS at the arrival time combined with

Table 3. Basic statistics for average PWAT and AR among 58 records.

Variables (all inner area)	N	Max.	Min.	Mean	Std. Dev.
Average PWAT 6 hours pre-arrival	58	67.154	39.257	56.69	8.293
Average PWAT 3 hours pre-arrival	58	62.371	0.012	22.144	22.86
Average PWAT	58	68.536	40.158	57.054	7.769
Average PWAT 3 hours post-arrival	58	63.769	0.026	22.483	23.432
Average PWAT 6 hours post-arrival	58	68.022	37.372	57.357	8.514
Average AR 6 hours pre-arrival	58	46.696	0	11.385	10.743
Average AR 3 hours pre-arrival	58	64.265	8.033	45.863	18.234
Average AR	58	32.36	0.006	10.289	10.145
Average AR 3 hours post-arrival	58	68.485	1.28	44.728	20.354
Average AR 6 hours post-arrival	58	28.542	0	6.48	8.05

Table 4. Results from regression analysis with different dependent variables and only one independent variable, maximum wind speed (Confidence level = 95%).

Inner Area AR Variables	Constant	N	R ²	F-ratio	K-S	S-W	A-D
Average	yes	56	0.783	199.15	0.123	0.41	>0.15
	no	57	0.857	336.55	0.004	0.002	<0.01
Accumulated	yes	57	0.756	174.103	0.215	0.61	>0.15
	no	58	0.85	323.809	0.002	0	<0.01
Average 3 hours post-arrival	yes	58	0.693	129.819	0.001	0.003	<0.01
	no	58	0.799	227.286	0	0	<0.01
Accumulated 3 hours post-arrival	yes	54	0.699	123.913	0.018	0.005	<0.01
	no	54	0.82	240.966	0.002	0	<0.01
Average 6 hours post-arrival	yes	52	0.73	139.167	0.029	0.011	<0.01
	no	53	0.772	175.867	0	0	<0.01
Accumulated 6 hours post-arrival	yes	47	0.856	274.873	0.002	0.027	<0.01
	no	54	0.768	175.517	0	0	<0.01

total amounts of AR and PWAT three hours prior (sumAR1a3 and sumPW1a3) estimated the average AR better than MWS alone. The total rainfall was greatly influenced by MWS and average PWAT six hours prior (avgPWI).

Repeated Measures Analysis

We divided each of the 58 records utilized for the regression analysis into 5 sub-records by time, and assigned the values of -6, -3, 0, 3 and 6 to the position six and three hours prior to arrival, at the arrival, and three and six hours after the arrival at each given storm center location, respectively. The basic statistics are found in Table 9. We set the binary variable GEO as 0 when the storm centers were over the ocean and as 1 when over land. The basic descriptive statistics of the new dataset are shown in Table 11. Pearson Product Moment Correlation (Pearson’s correlation) was utilized to observe the correlations between each pair of variables (Table 10).

We observed a significant positive correlation between PWAT and AR at a 95% confidence level, which further confirmed the potential of PWAT to predict the amount of AR. The AR was significantly negatively correlated with GEO at the 95% confidence

level, which implies that AR was significantly influenced by the geographical location of storm centers for each of the three hurricanes in our study. With 0 representing hurricanes while over the ocean and 1 over land, the amount of AR decreased after the landfall of the storm center, but not before. From the repeated measurement, we also found that during the 12 hours centered on the arrival time of storm centers at a given location, the rate of change of AR within a given inner area varied. The intensity of rainfall changed more slowly over land than over ocean (*p*-value=0.0215), despite lower amounts of AR over land after landfall.

DISCUSSION

In this study, GIS, regression analysis, and repeated measures analysis were used together to analyze the relationships between AR and PWAT within a given inner area of 111 km around the storm center, during the 72 hours centered at the arrival time of each storm at each location. In the inner areas, the MWS at the arrival time of storm centers alone provided better estimations for the total AR at

Table 5. Results from regression analysis for the average and total accumulated rainfall within inner areas at the arrival time of storm centers (Confidence level = 95%).

Dependent (inner area)	Independent (pre-arrival)	N	R ²	F-ratio	K-S	S-W	A-D
Average AR	constant, average inner area AR 3 hours, MWS	57	0.812	122.266	0.001	0.022	<0.01
	average inner area PW and AR 3 hours, MWS	57	0.909	186.098	0.001	0.041	<0.01
	constant, accumulated inner area AR 3 hours, MWS	56	0.804	113.978	0.001	0.009	<0.01
	accumulated inner area PW and AR 3 hours, MWS	56	0.905	174.516	0.003	0.018	<0.01
	constant, MWS	56	0.783	199.15	0.123	0.41	>0.15
	average outer area PW 3 hours, MWS	56	0.895	234.954	0.542	0.637	>0.15
	accumulated outer area PW 3 hours, MWS	56	0.895	234.845	0.181	0.326	>0.15
	average inner area PW 6 hours, MWS	56	0.897	240.722	0.417	0.649	>0.15
	accumulated inner area PW 6 hours, MWS	56	0.898	242.656	0.072	0.367	>0.15
	average outer area PW 6 hours, MWS	56	0.897	240.58	0.393	0.716	>0.15
accumulated outer area PW 6 hours, MWS	56	0.897	239.812	0.14	0.365	>0.15	
Accumulated AR	constant, average inner area AR 3 hours, MWS	57	0.775	97.606	0.006	0.114	0.031
	average inner area PW and AR 3 hours, MWS	57	0.895	158.937	0.041	0.166	0.062
	constant, accumulated inner area AR 3 hours, MWS	57	0.787	104.2	0.004	0.099	<0.01
	accumulated inner area PW and AR 3 hours, MWS	57	0.901	170.139	0.031	0.131	0.015
	constant, MWS	57	0.756	174.103	0.215	0.601	>0.15
	average outer area PW 3 hours, MWS	57	0.884	212.878	0.29	0.697	>0.15
	accumulated outer area PW 3 hours, MWS	57	0.887	220.171	0.358	0.637	>0.15
	average inner area PW 6 hours, MWS	57	0.886	217.741	0.566	0.664	>0.15
	accumulated inner area PW 6 hours, MWS	57	0.89	227.319	0.214	0.611	>0.15
	average outer area PW 6 hours, MWS	57	0.886	218.39	0.485	0.746	>0.15
accumulated outer area PW 6 hours, MWS	57	0.889	225.592	0.345	0.684	>0.15	

that moment (sumARI). MWS also provided reasonable predictions for each of the other five dependent variables (avgARI, avgAR1a3, sumAR1a3, avgAR1a6 and sumAR1a6). However, these five dependent variables were predicted more accurately when involving AR- and PWAT-related variables occurring three and six hours earlier than dependent variables.

The goal of this study was to improve short-term forecast of rainfall after hurricanes. The temporal resolution of the data is higher than the previous study (Jiang, Halverson and Zipser 2008), where the authors interpolated moisture data into 3-hour increments from a 12-hour temporal resolution with a 111×111 km² spatial resolution. While it is difficult to predict the total amount of rain-

Table 6. Results from regression analysis for the average and total accumulated rainfall within inner areas three hours after the arrival time of storm centers (Confidence level = 95%).

Dependent (inner area)	Independent (pre-arrival)	N	R ²	F-ratio	K-S	S-W	A-D
Average AR 3 hours post-arrival	constant, average inner area AR, MWS	58	0.767	95.056	0.007	0.039	<0.01
	average inner area PW and AR, MWS	58	0.878	137.049	0.012	0.043	0.012
	constant, accumulated inner area AR, MWS	57	0.828	135.354	0.027	0.153	0.042
	accumulated inner area AR	57	0.897	488.963	0.009	0.022	<0.01
	constant, MWS	58	0.693	129.819	0.001	0.003	<0.01
	average inner area PW 3 hours, MWS	58	0.835	145.075	0	0.007	<0.01
	accumulated outer area PW, MWS	58	0.838	148.461	0.015	0.012	<0.01
	average inner area PW 3 hours, MWS	58	0.835	144.547	0.001	0.005	<0.01
	accumulated inner area PW 3 hours, MWS	58	0.839	149.119	0.016	0.008	<0.01
	average outer area PW 3 hours, MWS	58	0.832	142.093	0	0.004	<0.01
	accumulated outer area PW 3 hours, MWS	58	0.836	145.523	0.013	0.01	<0.01
Accumulated AR 3 hours post-arrival	constant, average inner area AR, MWS	58	0.69	64.577	0	0.004	<0.01
	average inner area AR, MWS	58	0.831	140.264	0	0	<0.01
	constant, accumulated inner area PW and AR	57	0.815	124.518	0.293	0.228	0.112
	accumulated inner area AR	57	0.879	407.791	0	0.004	<0.01
	constant, MWS	54	0.699	123.913	0.018	0.005	<0.01
	average inner area PW 3 hours, MWS	54	0.843	142.943	0.007	0.005	<0.01
	accumulated inner area PW 3 hours, MWS	54	0.851	151.371	0.017	0.012	<0.01

fall produced by hurricanes prior to arrival, AR- and PWAT-related variables can be accurately gauged by satellite at any given place and provide approximate estimations for the average and total amounts of AR after three and six hours. It is important to note that the average and total amount are more stable and easier to predict than the maximum and minimum. Theoretically, the PWAT in the air

needs several hours to transfer to the ground, so an appropriate time lag between PWAT and AR data is crucial for forecast purposes and produces better predictions than MWS does alone.

Due to friction with land, a lack of warm water convection to support storm development, and subsequent weakening of the hurricane, there were lower amounts of rainfall

Table 7. Results from regression analysis for the average and total accumulated rainfall within inner areas six hours after the arrival time of storm centers (Confidence level = 95%).

Dependent (inner area)	Independent (post-arrival)	N	R²	F-ratio	K-S	S-W	A-D
Average AR 6 hours post-arrival	constant, average inner area PW and AR 3 hours, MWS	50	0.866	106.293	0.045	0.097	0.015
	average inner area PW and AR 3 hours, MWS	50	0.916	178.12	0.042	0.094	0.013
	constant, accumulated inner area AR 3 hours, MWS	56	0.723	72.67	0	0	<0.01
	accumulated inner area PW 3 hours, accumulated inner area AR 3 hours, MWS	56	0.831	91.133	0.001	0.001	<0.01
	constant, average inner area PW, MWS	49	0.833	120.758	0.182	0.138	0.068
	average inner area PW, MWS	49	0.896	207.467	0.092	0.043	0.011
	constant, accumulated inner area PW, MWS	58	0.622	47.924	0.044	0.001	<0.01
	accumulated inner area PW, MWS	53	0.839	136.474	0.111	0.124	0.034
Accumulated AR 6 hours post-arrival	constant, average inner area AR 3 hours, MWS	50	0.865	158.264	0.161	0.13	0.046
	average inner area PW and AR 3 hours, MWS	50	0.924	198.894	0.071	0.039	<0.01
	constant, accumulated inner area AR 3 hours, MWS	50	0.855	145.105	0.154	0.432	0.14
	accumulated inner area PW and AR 3 hours, MWS	50	0.914	173.917	0.237	0.442	>0.15
	constant, average inner area PW, MWS	47	0.885	178.137	0.051	0.222	0.064
	average inner area PW, MWS	47	0.93	306.156	0	0.029	<0.01
	constant, accumulated inner area PW, MWS	54	0.72	69.038	0.15	0.136	0.082
	accumulated inner area PW, MWS	53	0.837	133.812	0	0.004	<0.01

over land than over the ocean. However, the rate of change was slower over land, which caused the vulnerable populations living near landfall and around storm centers to be exposed to flooding for a longer period of time. It is not always the case that hurricanes will slow their forward movement after landfall. Latitude is one of many important factors in determining whether a hurricane accelerates after making landfall (Coch 1994). In most situations, including the three hurricanes in our study, there was little to no increase in forward acceleration after making landfall at

lower latitudes. Heavy flooding often results from a slow tracking storm moving across the lower latitudes of the U.S.A., although this is not always the case since heavy flooding has occurred in the northeastern U.S.A. from faster moving storms (e.g., Hurricane Irene in 2011).

The underlying physical mechanisms behind the relationships between AR- and PWAT-related variables warrant further meteorological study, but we are able to conclude the importance of the PWAT. When the storms approach, the flooding situations

Table 8. Comparison of adjusted R^2 before and after involving AR- and PWAT-related variables in the models.

Variables (all inner area)	Old	New	Improvement
Average AR	0.857	0.909	0.052
Accumulated AR	0.85	0.787	-0.063
Average AR 3 hours post-arrival	0.799	0.897	0.098
Accumulated AR 3 hours post-arrival	0.82	0.879	0.059
Average AR 6 hours post-arrival	0.772	0.831	0.059
Accumulated AR 6 hours post-arrival	0.856	0.93	0.074

Table 9. Basic statistics for 290 sub-records.

Basic Statistics						
Variable	N	Mean	Std. Dev.	Sum	Min.	Max.
STORM	290	2.22	0.79	645	1	3
TIME	290	0	4.25	0	-6	6
AR	290	10.38	10.51	3009	0	52.86
PWAT	290	56.52	8.24	16390	31.21	68.54
GEO	290	0.55	0.5	160	0	1

Table 10. Pearson correlation coefficients.

Pearson Correlation Coefficients, N = 290 Prob > r under H0: Rho=0			
	AR	PWAT	GEO
AR	1	0.48639 <.0001	-0.48517 <.0001
PWAT	0.48639 <.0001	1	-0.10215 0.0824
GEO	-0.48517 <.0001	-0.10215 0.0824	1

after three to six hours can be approximately predicted, and populations exposed to flooding may be effectively protected or evacuated ahead of time, based on the severity of the situations. The focus of this study is the inner areas around storm centers. We defined the AR- and PWAT-related variables within outer areas for the purpose of observing whether

these variables are able to explain the amount of rainfall within inner areas. Nonetheless, none of the variables within outer areas have been found to be significantly correlated with any target dependent variable.

The limited number of hurricanes and variables involved provide only a small, but effective, sample for our study. Some errors may

originate from the satellite-derived data and Kriging interpolation. For instance, GPROF selected different channels and strategies for measurements over land and ocean, resulting in a -17% positive bias over land, compared with rain gauge data, and -9% negative bias over the ocean (Jiang, Halverson and Zipser 2008). Additionally, it is worth noting that there is a bias between accurate and hypothesized time of landfall. For future studies, a larger group of hurricanes could be used and more variables incorporated for more conclusive predictions. Regardless, our study indicates that the amount of rainfall produced by hurricanes can be predicted with some level of accuracy based on rainfall and moisture amounts three and six hours prior to arrival in specific locations.

NOTES

1. Coordinated Universal Time (UTC) is the primary time standard by which the world regulates clocks and time.

REFERENCES

- Akkala, A., V. Devabhaktuni, and A. Kumar. 2010. Interpolation techniques and associated software for environmental data. *Environmental Progress & Sustainable Energy* 29(2):8.
- Carr, F. H., and L. F. Bosart. 1978. A diagnostic evaluation of rainfall predictability for Tropical Storm Agnes, June 1972. *Monthly Weather Review* 106(3):363-74.
- Coch, N. K. 1994. Hurricane hazards along the northeastern Atlantic coast of the United States. *Journal of Coastal Research*:115-47.
- Demuth, J. L., M. DeMaria, and J. A. Knaff. 2006. Improvement of advanced microwave sounding unit tropical cyclone intensity and size estimation algorithms. *Journal of Applied Meteorology and Climatology* 45(11):1573-81.
- DiMego, G. J., and L. F. Bosart. 1982. The transformation of Tropical Storm Agnes into an extratropical cyclone. Part II: Moisture, vorticity and kinetic energy budgets. *Monthly Weather Review* 110(5):412-33.
- Elsberry, R. L. 2002. Predicting hurricane landfall precipitation: Optimistic and pessimistic views from the symposium on precipitation extremes. *Bulletin of the American Meteorological Society* 83(9):1333-39.
- Inc., SAS Institute. 1999. *The Analyst Application*, First Edition.
- Jiang, H., J. B. Halverson, and J. Simpson. 2008. On the differences in storm rainfall from hurricanes Isidore and Lili. Part I: Satellite observations and rain potential. *Weather and Forecasting* 23(1):29-43.
- Jiang, H., J. B. Halverson, J. Simpson, and E. J. Zipser. 2008a. Hurricane rainfall potential derived from satellite observations aids overland rainfall prediction. *Journal of Applied Meteorology and Climatology* 47(4):944-59.
- _____. 2008b. On the differences in storm rainfall from Hurricanes Isidore and Lili. Part II: Water budget. *Weather and Forecasting* 23(1):44-61.
- Jiang, H., J. B. Halverson, and E. J. Zipser. 2008. Influence of environmental moisture on TRMM-derived tropical cyclone precipitation over land and ocean. *Geophysical Research Letters* 35(17).
- Kummerow, C., W. S. Olson, and L. Giglio. 1996. A simplified scheme for obtaining precipitation and vertical hydrometeor profiles from passive microwave sensors. *Geoscience and Remote Sensing, IEEE Transactions* 34(5):1213-32.
- Li, L., and P. Revesz. 2004. Interpolation methods for spatio-temporal geographic data. *Computers, Environment and Urban Systems* 28(3):201-27.
- Lonfat, M., R. Rogers, T. Marchok, and F. D. Marks Jr. 2007. A parametric model for predicting hurricane rainfall. *Monthly Weather Review* 135(9):3086-97.
- Moser, E. B. 2004. Repeated measures modeling with PROC MIXED. *Proceedings of the 29th SAS Users Group International Conference*:9-12.
- Oliver, M. A., and R. Webster. 1990. Kriging: a method of interpolation for geographical

- information systems. *International Journal of Geographical Information System* 4(3):313-32.
- Olson, W. S., C. D. Kummerow, Y. Hong, and W. K. Tao. 1999. Atmospheric latent heating distributions in the tropics derived from satellite passive microwave radiometer measurements. *Journal of Applied Meteorology* 38(6):633-64.
- Tootle, G. A., T. Mirti, and T. C. Piechota. 2005. Magnitude and return period of 2004 hurricane rainfall in Florida. *Journal of Floodplain Management* 5(1):32.